Understanding metal oxide/water interaction from first principles calculations

Giacomo Melani, Steven Lindner, Eric Fischer and Peter Saalfrank

April 25, 2019

Project Leader:

Prof. Dr. Peter Saalfrank
Universität Potsdam, Institut für Chemie
Karl-Liebknecht-Straße 24-25, 14476 Potsdam
Tel.: +49-331-977-5232
Fax: +49-331-977-5058
Email: peter.saalfrank@uni-potsdam.de

Project administrator:

Giacomo Melani
Universität Potsdam, Institut für Chemie
Karl-Liebknecht-Straße 24-25, 14476 Potsdam
Tel.: +49-331-977-5230
Fax: +49-331-977-5058
Email: melanie@uni-potsdam.de

The project of this fourth, and last continuation proposal for bbc00001 is connected to the Collaborative Research Centre (CRC) 1109 ("Understanding of Metal Oxide/Water Systems at the Molecular Scale", subproject Campen/Saalfrank), whose funding period finished in December 2018. This proposal is therefore meant to be a summary of research works conducted within the last year(s), and to describe further work which is desirable to conclude our investigation.

1 Introduction and scientific context

In the last four years, our group has been deeply involved in a joint theoretical and experimental project, designed to study water on metal oxide surfaces. Specifically, our efforts have been spent to describe water reactivity and interactions towards aluminum oxide, in its α-Al_2O_3 form, also known as α-alumina. In collaboration with experimental partners ("Interfacial Molecular Spectroscopy" group, Department of Physical Chemistry, Fritz-Haber Institute of MPG, Berlin), we have unravelled water adsorption on various surfaces of α-Al_2O_3, among which the (0001) termination has been investigated from low to medium coverage regimes. In particular, to study water

(D_2O) molecular or dissociative adsorption, the Al-terminated (0001) surface has been considered, which is the most stable structure in UHV conditions. On the other hand, to describe a higher coverage picture, the first step towards simulation of the solid / liquid interface, a reconstructed hydroxylated O-terminated (0001) surface has been examined, with and without additional water. The latter is known to be the most stable termination in aqueous environmental conditions.

In the last funding period, our attention has been focused on integrating the information gained experimentally with surface-sensitive Vibrational Sum Frequency (VSF) generation spectroscopy, both in terms of spectroscopic assignment and of description of dynamical processes investigated by pump-probe experiments. As in the preceeding funding period, our theoretical approach is based on periodic Density Functional Theory (DFT) calculations at the GGA level of theory and on Ab Initio Molecular Dynamics (AIMD) simulations.

Here we summarize our latest results within our project bbc00001 achieved in the last year (4th funding period), focused on two main issues:

- Description of vibrational energy relaxation processes for interfacial OH species on water-covered hydroxylated α-Al_2O_3(0001) surface by means of non-equilibrium AIMD, in close connection with vibrational lifetimes obtained from time-resolved VSF measurements.
- Theoretical treatment of vibrational spectra of dissociated D_2O on Al-terminated α-Al_2O_3(0001) surface using time-correlation functions from AIMD trajectories, beyond previous results based on static Normal Mode Analysis (NMA). The calculated spectra were tested against experimental VSF data.

The work related to both subprojects has presented in recent publications or are in the process of being published, as listed in Sec. 5.

2 Progress Report

In all our investigations we solve the Kohn-Sham equations [1] of DFT, using the Vienna Ab initio Simulation Package (VASP) [2, 3], using the Perdew Burke Ernzerhof exchange-correlation functional (PBE) [4], a projector-augmented plane wave (PAW) basis [5, 6], and Grimme's D2 correction [7] for dispersive interactions. Further numerical details can be found in Refs. [8,9]. For AIMD simulations, nuclear trajectories have been propagated in the canonical (NVT) ensemble at finite temperature using the Nosé-Hoover thermostat [10].

In the entire project, three subprojects have been formulated so far:

- Subproject 1: MBS modelling of water dissociation on Al-terminated $\boldsymbol{\alpha}$-Al_2O_3(0001)

- Subproject 2: Water thin-film structures and vibrational dynamics at OH-terminated α-$Al_2O_3(0001)$
- Subproject 3: Vibrational spectroscopy of dissociated D_2O at Al-terminated α-Al_2O_3 surfaces

The first one has been finished and was reported in previous progress reports. The present progress report focuses on subprojects 2 and 3.

2.1 Subproject 2: Water thin-film structures and vibrational dynamics at OH-terminated α-$Al_2O_3(0001)$

One goal of our project consists of the interpretation *via* computational methods of time-resolved VSF spectroscopy experiments, performed by our partners at FHI. In these experiments, an infrared laser pulse centered at 3710 cm^{-1} is used to excite selectively a surface mode within the water / α-$Al_2O_3(0001)$ interface. Given the vibrational signatures obtained by static NMA as well as by AIMD simulations [11], we have chosen what we call the HS+2ML system as a model to mimic intermediate water coverages. The HS+2ML stands for a hydroxylated α-alumina surface model, terminated by OH-bonds, where the (0001) surface is covered by eight additional water molecules ("2 ML", monolayers), as shown in Fig.1. Please see Ref. [11] for detailed information about the structure.

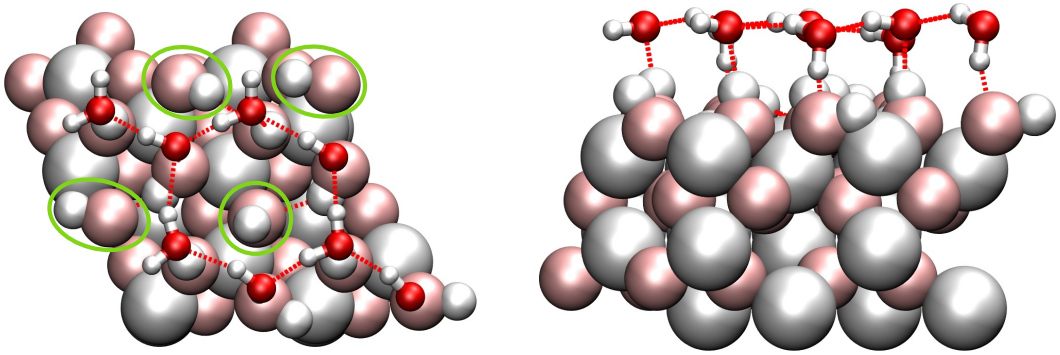

Figure 1: Top (left) and side views (right) of the hydroxylated α-$Al_2O_3(0001)$ surface (2×2), with additional eight water molecules (HS+2ML). Our model has a stoichiometric composition of 92 atoms ($Al_{20}O_{36}H_{12} \cdot (H_2O)_8$). Surface atoms are shown as "van-der-Waals spheres" in pale colors, water thin films in a "ball-and-stick" representation (H in white, Al in grey and O in red). Hydrogen bonds are indicated by dashed red lines. In AIMD, only the upermost two atomic layers (an O layer and a double-layer of Al) plus the adsorbate atoms were allowed to move, while the lower layers were kept frozen at bulk geometries. Encircled in green are the non-hydrogen bonded OH-bonds (aluminols) which are perturbed in non-equilibrium dynamics.

The choice of this model was mostly motivated by experimental findings, since our colleagues obtained vibrational lifetimes for the α-$Al_2O_3(0001)$ surface of: 3.3 ps (measurements in contact with air) and 3.5 ps (measurements in contact with liquid water). These results suggested the very first layer(s) of water molecules adsorbed on a hydroxylated surface of being "de-coupled" from bulk water. Previous calculations by our group, already presented in previous proposals, have tried to reproduce the IR-induced dynamics in order to obtain experimentally observed relaxation times. However, the computational strategy previously used was based on shorter AIMD trajectories (maximum ten picoseconds) and on a realization of vibrational excitation by displacement of a single interfacial O-H bond. In the last funding period we decided to redesign this part of subproject 2, using a more refined and efficient non-equilibrium molecular dynamics scheme. The full "*equilibrium + non-equilibrium*" AIMD approach is schematically reported in Fig.2 and consists of the following steps:

- Geometry optimization at the PBE+D2 level of theory of initial HS+2ML structure.
- Canonical NVT / AIMD trajectories at 300 K: five trajectories each 24 ps long (*Equilibration*).
- Microcanonical NVE / AIMD trajectories starting from the previous one at finite temperature: five trajectories each 10 + 10 ps long (*Post-equilibration*).
- Microcanonical NVE / AIMD trajectories after "swapping" of nuclear velocities of specific O-H bonds: two sets (NEQ_1, NEQ_2) of five trajectories each 10 ps long (*Non-equilibrium phase*).

Overall, a total of 320 ps of DFT-based *ab initio* molecular dynamics simulations have been calculated, 120 of which for equilibration at 300 K, 100 ps for post-equilibration within the microcanonical ensemble and other 100 ps for non-equilibrium dynamics.

Let us now focus on stage (3) of the scheme in Fig.2, when nuclear velocities of selected O-H bonds associated with interfacial aluminols are "swapped" [12]. The interaction of a vibrational chromophore with Infrared light normally involves the absorption of a vibrational quantum of energy, $\hbar\omega_{10} \sim 0.46$ eV, as the exciting pulse is resonant with the energy difference between ground and first vibrationally excited state. Such excessive energy brought by the electromagnetic perturbation is assumed in our AIMD scheme to generate a kinetic energy contribution which is added to the "ground-state" kinetic energy of selected aluminols. In this way, swapping of nuclear velocities enables us to perform *non-equilibrium* simulations, without the need of more complex techniques (*i.e.*, explicit coupling with an Infrared pulse). Of course, the excess of energy stored in the O-H bonds at stage (3) will be rapidly redistributed to other modes – relaxation takes place. In our approach, the excitation of interfacial aluminols is done as follows. We select only non-hydrogen-bonded, upright aluminols as the ones to be perturbed in the *non-equilibrium* AIMD scheme of

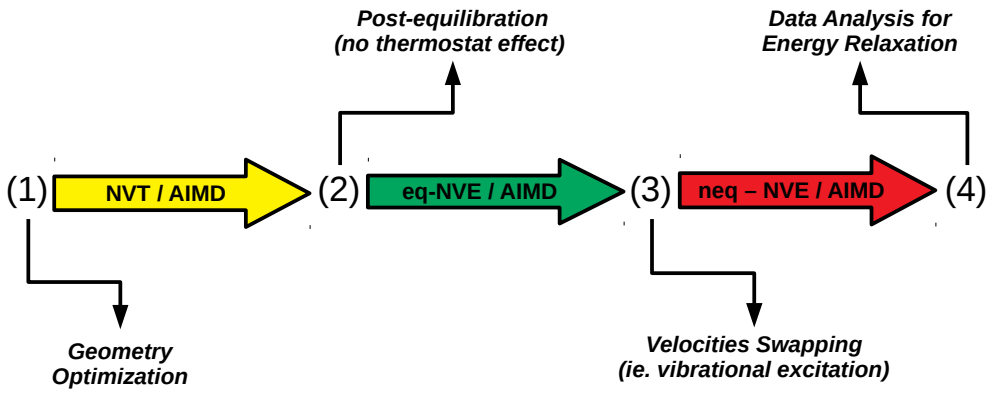

Figure 2: Schematic representation of non-equilibrium AIMD protocol: at the very beginning, (1) the initial HS+2ML structure is optimized at the PBE+D2 level of theory. Then, canonical *ab initio* molecular dynamics (NVT / AIMD) trajectories at 300 K are propagated until thermal equilibrium is reached. At (2), AIMD trajectories are further propagated within the microcanonical ensemble to remove any spurious effect caused by coupling with the thermostat. This phase consists in a "post-equilibration". After a certain amount of time, nuclear velocities of specific O-H bonds are changed (3). Here, a "non-equilibrium" phase begins during the course of which excited O-H kinetic energies are monitored. Eventually, at (4) full data analysis is performed to dissect vibrational relaxation process.

Fig.2. The following criterion comes then into play: at step (3), post-equilibrated NVE / AIMD trajectories are analyzed and polar angles of all non-hydrogen-bonded aluminols are calculated at $t = 0$, if polar angle is larger than 45° the nuclear velocities of the considered aluminol are swapped and the bond excited, otherwise the bond is left unperturbed. According to this method, not all four non-hydrogen-bonded aluminols are excited at step (3), but only the ones that are upright at that moment. Eventually, in both sets of non-equilibrium AIMD trajectories, NEQ_1 and NEQ_2, we retrieve that, on average, around three aluminols get perturbed.

In the following, results from the non-equilibrium AIMD trajectories are reported, concerning the evolution of excited non-hydrogen-bonded aluminols from the HS+2ML system shown in Fig.1. We shall first do a detailed analysis of the time evolution of the kinetic energy before and after the velocities swapping. As we can observe in Fig.3, both sets of AIMD trajectories NEQ_1 and NEQ_2 are characterized by an initial equilibrium phase which is then perturbed by the excessive kinetic energy in the selected non-hydrogen bonded aluminols. In order to disentangle the role of different pathways for energy redistribution, we reported averaged E_{kin} values for different subsystems of HS+2ML, namely: the four non-hydrogen bonded aluminols, among which we find the excited up-

right bonds, the hydrogen-bonded aluminols, the water molecules forming the adsorbed layer and the remaining surface atoms. This simple structural criterion allows us already to observe which of the different degrees of freedom participate in the kinetic energy redistribution after vibrational excitation. As it is seen from Fig.3, in both NEQ_1 and NEQ_2 sets the average kinetic energy of non-hydrogen-bonded aluminols after the post-equilibrium phase (10 ps or 20 ps long) manifests a sudded increase by nearly 1.4 eV, which is consistent with the average number of around three excited bonds for AIMD trajectory. The E_{kin}^{nhb-OH} stored in the excited bonds then gradually decreases within the 10 ps employed to propagate the non-equilibrium trajectories, until the initial excess of kinetic energy is redistributed. Dissecting the total E_{kin} into the different subsystems allows us to notice that both neighboring water molecules and hydrogen-bonded aluminols seem to be the effective channels for vibrational energy dissipation. In fact, the average E_{kin} values for water layer and hb-OH bonds appear to increase rapidly within the first 2-3 ps after vibrational excitation to then reach a new equilibrium value after 5 ps. On the other hand, surface atoms seem to increase their kinetic energy more slowly and appreciably only after 5-6 ps from the beginning of the non-equilibrium dynamics.

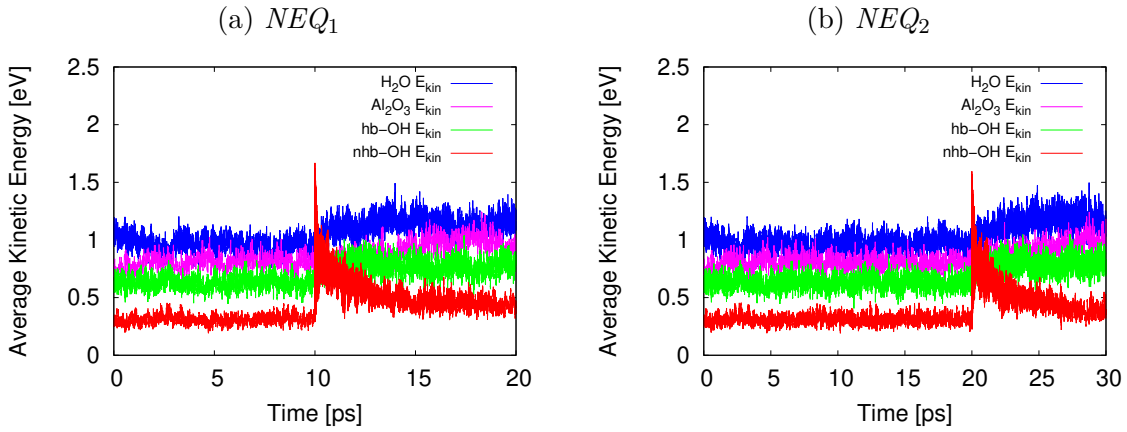

Figure 3: Average Kinetic Energy associated with different subsystems of HS+2ML: *nhb-OH* as the non-hydrogen-bonded aluminols (among which there are the excited ones), *hb-OH* as the hydrogen-bonded aluminols; H_2O and Al_2O_3 being associated with kinetic energies of water layer and surface atoms, respectively.

The effective relaxation dynamics appears clearer thanks to the graphs reported in Fig.4. Here, we employ a "system + bath" picture, where the non-hydrogen-bonded aluminols are taken as excited (sub)system, while the whole "hydrogen-bonded aluminols + water layer + surface atoms" ensemble is taken as accepting thermal bath. The two graphs in upper and lower panels of Fig.4 depict a clear quasi-exponential decay for excited aluminols (*system*), while the average *bath* kinetic energy follows an incremental trend which reaches a new steady-state condition within the last picoseconds of the non-equilibrium AIMD trajectories. A possible way to compute vibrational

lifetimes for the O-H stretching modes, which have been probed experimentally, is *via* interpolating the decaying average kinetic energy of non-hydrogen-bonded aluminols with an exponential curve. Using a fitting curve for the kinetic energy of the non-hydrogen bonded OH groups,

$$E_{kin}^{nhb-OH}(t) = E_{kin}^{nhb-OH}(0)e^{-t/\tau_{OH}} + \delta(E_{kin}^{nhb-OH}) \tag{1}$$

we get τ_{OH} as the relaxation time and $\delta(E_{kin}^{nhb-OH})$ as the long-time limit of aluminols' kinetic energy after relaxation. The resulting fits give relaxation times of 1.8 and 2.3 ps, for the two sets NEQ_1 and NEQ_2 respectively. These results are already in qualitative agreement with experimental values.

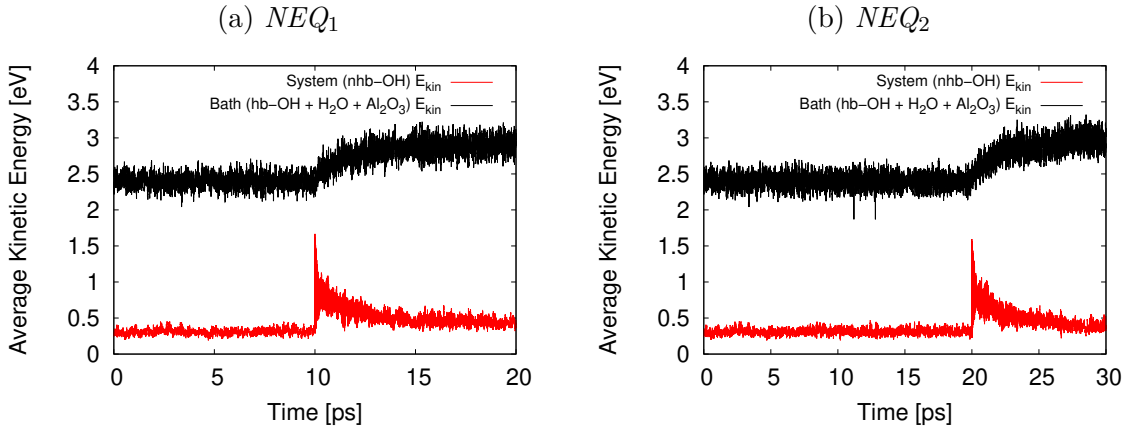

Figure 4: Average Kinetic Energy partitioned as "*system* + *bath*", where the *system* is associated with non-hydrogen-bonded aluminols, and the *bath* with the sum of hydrogen-bonded aluminols, water layer and surface contributions.

The analysis based on kinetic energy decay suffers from two main defects, one methodological and one more physical. From the methodological, or technical, side we notice that E_{kin} data appear quite noisy given the consistent amount of data points we obtain from AIMD trajectories. Another analysis proposed in Refs. [13, 14] suggests to employ so-called "Kinetic Energy Spectral Densities" as obtained *via* first Fourier transform of properly mass-scaled velocity-velocity autocorrelation functions, which are initially truncated after a certain time interval and so are then back-transformed in the time domain as instantaneous kinetic energies. A similar procedure has been proposed by Lesnicki *et al* [15], but here the computed spectral densities are directly obtained by the velocity-velocity (auto)correlation functions. In fact, the analysis of vibrational energy relaxation within our HS+2ML model can be based on looking how Vibrational Densities of States (VDOS) of selected subsystems evolve in time. A VDOS is calculated directly as a real part of the Fourier-transformed velocity-velocity autocorrelation functions. While for equilibrium dynamics, the correlation functions are usually sampled from the last segment of AIMD trajecto-

ries, in non-equilibrium AIMD the initial time from which the VVAF is calculated can be tuned. We can therefore have Vibrational Densities of States that depend on different time intervals of the non-equilibrium trajectories, $VDOS(\omega, t)$. With such approach we can resolve the evolution of our vibrational spectral densities within the 10 ps of the non-equilibrium phase in order to follow the vibrational relaxation of excited aluminols in both time- and frequency-domains. In the following analysis, we sample the VVAFs for 1 ps and the time origin t is shifted from 0 to 9 ps.

(a) NEQ_1, full

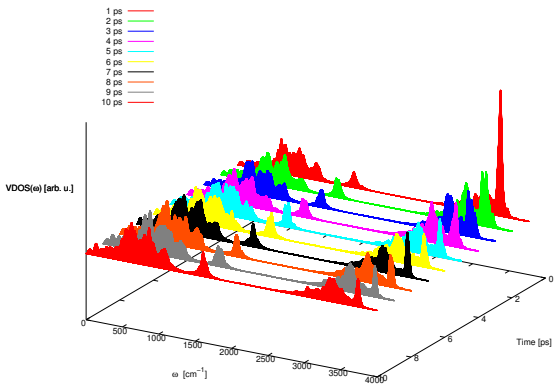

(b) NEQ_2, full

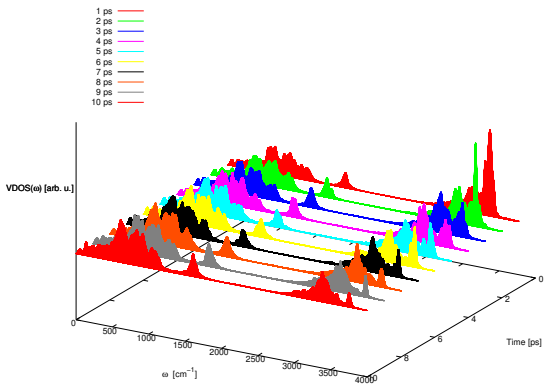

(a) NEQ_1, zoom

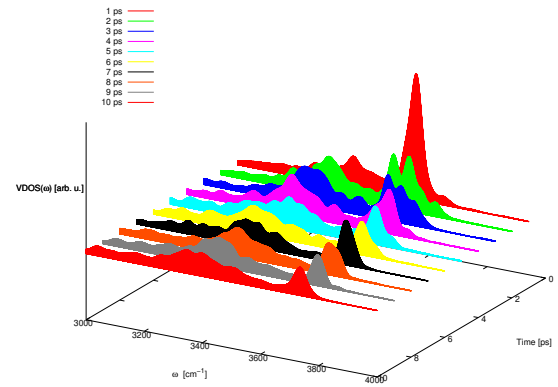

(b) NEQ_2, zoom

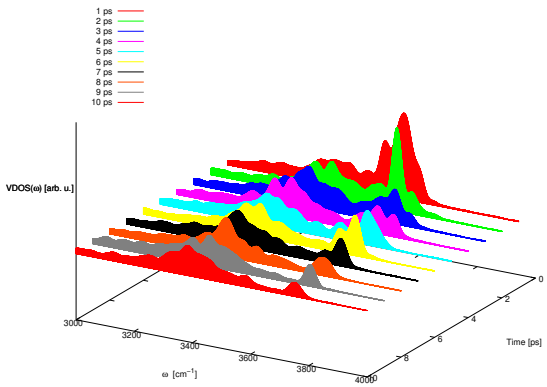

Figure 5: Time-evolution of Vibrational Density of States for the total HS+2ML system in the two sets of non-equilibrium AIMD simulations, NEQ_1 (a) and NEQ_2 (b). The legend indicates the time shift from the beginning of non-equilibrium trajctories (t = 0). Upper panels show full VDOS spectra, while lower panels show a closer look at O-H stretching frequencies between 3000 and 4000 cm^{-1}.

Let us look at the time evolution of $VDOS(\omega, t)$ calculated following the course of the non-equilibrium dynamics, as shown in Fig.5. Already looking at the spectral density of the total HS+2ML system, we can appreciate a highly intense peak around 3600 cm^{-1} at the beginning of the non-equilibrium AIMD. This peak in the VDOS at 1 ps arises from the vibrationally excited

non-hydrogen bonded aluminols and its position at lower frequencies (not centered at 3750 cm^{-1} as we would have expected in equilibrium conditions) can be explained by taking into account both the anharmonicity of the O-H bond and the classical motion of nuclei [13, 14]. Due to the continous and almost instantaneous exchange between kinetic and potential energy, anharmonicity then causes a redshift of the oscillation frequency of the excited O-H bonds. During the relaxation process, the excited bonds will be effected both by a gradual blueshift towards their vibrational frequency at thermal equilibrium and a loss of their kinetic energy, indicated by less intense peaks in the $VDOS(\omega, t)$ plots. This effect is clearly visible in the VDOS region between 3000 and 4000 cm^{-1} of Fig.5 (lower panels).

To summarize, the analysis of both kinetic energy and Vibrational Densities of States provide semi-quantitative tools to unravel the energy dissipation of excited upright non-hydrogen bonded aluminols, which were the main focus of this subproject. In this work, the analysis of non-equilibrium AIMD trajectories suggests that, once excited by a vibrational quantum in their kinetic energy, such non-hydrogen-bonded aluminols decay rapidly within the first picoseconds of propagation, with relaxation times that can be almost quantitatively obtained either *via* an exponential fit of their average kinetic energy or by looking at the time-evolution of their spectral densities. Both approaches suggest a "lifetime" between 2 and 4 ps. The tools we adopted also allow us to disentangle the role of other structural domains of the HS+2ML model in the relaxation process. Indeed, we can identify as main dissipative channels both hydrogen-bonded aluminols and, more importantly, water molecules from the adsorbed layer. Hydrogen-bonded modes, whose spectral signatures are identifiable in the region between 3000 and 3500 cm^{-1}, act as major pathways for the redistribution of the initial excess of kinetic energy. *These results are currently being prepared for a publication* (not yet listed in Sec.5).

2.2 Subproject 3: Vibrational spectroscopy of dissociated D_2O at Al-terminated α-Al_2O_3 surfaces

As reported in the preceeding project proposal, our group has recently acquired a new competence in the simulation of vibrational spectra from molecular dynamics calculations. In a collaboration with Dr. Yuki Nagata (Department of Molecular Spectroscopy, Max-Planck Institute for Polymer Research, Mainz), we etsablished an efficient methodology based on velocity-velocity autocorrelation functions (VVAFs) to obtain vibrational spectra (Vibrational Densities of States (VDOS), InfraRed (IR) and VSF) for hydroxylated α-alumina, highlighting the vibrational signatures in the OH stretching region depending on further water coverage and local hydrogen bonding environment [11]. The methodology we employed is based on a parametrization of O-H(D) transition dipole moment and polarizability, which makes it applicable to other aqueous interfaces, for instance to study vibrational responses of adsorbed D_2O on the Al-terminated α-alumina(0001)

surface. This system has been already object of study from our group [8, 9, 16], together with experimental partners. However, the interpretation of VSF spectroscopic signals had relied only on OD vibrational frequencies from NMA calculations. The latter suffer from several methodological drawbacks, among which the lack of anharmonicity, line broadening, (inter)mode coupling and finite-temperature effects as well as the absence of spectroscopic selection rules, hence of intensities. The VVAF-method adopted in Refs. [11, 17] allows to retrieve these effects and to directly simulate IR and VSF responses of OD species. Here we report a systematic analysis of vibrational frequencies from static NMA results and from AIMD-based correlation functions at finite temperature, 300 K. *This work has been submitted recently* (Ref.(D) in Sec.5).

In this work, low-coverage situations for water on Al-terminated α-Al_2O_3(0001) are studied. We use the Al-I surface model [18], same as in Refs. [8,9,16,19], comprising a 9-atomic layer (2×2) supercell (layer sequence Al_4-O_{12}-Al_4-Al_4-O_{12}-Al_4-Al_4-O_{12}-Al_4) with dimensions 9.66 Å×9.66 Å×31.41 Å (20 Å of vacuum in the z-direction), and employing 3D periodic boundary conditions. For geometry optimizations, NMA and AIMD the lowest four layers (Al_4-O_{12}-Al_4-Al_4) are kept fixed at bulk values optimized in Ref. [9], while the upper five layers (O_{12}-Al_4-Al_4-O_{12}-Al_4) are allowed to be relaxed, or to move. On top of this relaxed surface, which exhibits four Al CUS sites, water molecules are adsorbed and corresponding structures have been optimized.

Two coverages were considered. In a first model, we have one water molecule per (2×2) cell, *i.e.*, coverage 1/4. For the 1/4 coverage case, the corresponding, most stable dissociated species are those of Refs. [9,16,19], *i.e.*, the 1-2, 1-4, and 1-4' configurations shown in Fig.6(a)-(c). The molecular adsorbate corresponds also to a local minimum but is not shown here. Each dissociation mode (1-2, 1-4, 1-4') comprises two OD groups, a water-hydroxyl group which we denote as "adsorbate OD" in what follows, and an OD group consisting of a water-D plus a substrate O, "surface OD". 1-2 is found to be the most stable, 1-4 and the molecular species less but about equally stable on this level of theory, and 1-4' is slightly less stable than all the previous ones, in agreement with previous observations [9]. In order to study the effects of coverage, also the case with two molecules per (2×2) cell was considered, *i.e.*, coverage 1/2. Various combinations of dissociated and molecular adsorbed species and their adsorption sites are now conceivable. In Fig.6 we show PBE+D2 optimized structures obtained by simply doubling the optimized 1-2, 1-4 and 1-4' motifs of the monomer at a neighbouring Al CUS site, and reoptimizing. In this case, doubly-dissociated species are obtained which were as starting geometries for AIMD. We emphasize, however, that these doubly-dissociated dimer species are not necessarily the lowest-energy structures.

As a first step towards the characterization of vibrational modes for different dissociated D_2O structures on Al-terminated α-alumina (0001), we report calculated frequencies by NMA using PBE+D2 treatment at the optimized geometries of Fig.6. Since our main source of comparison

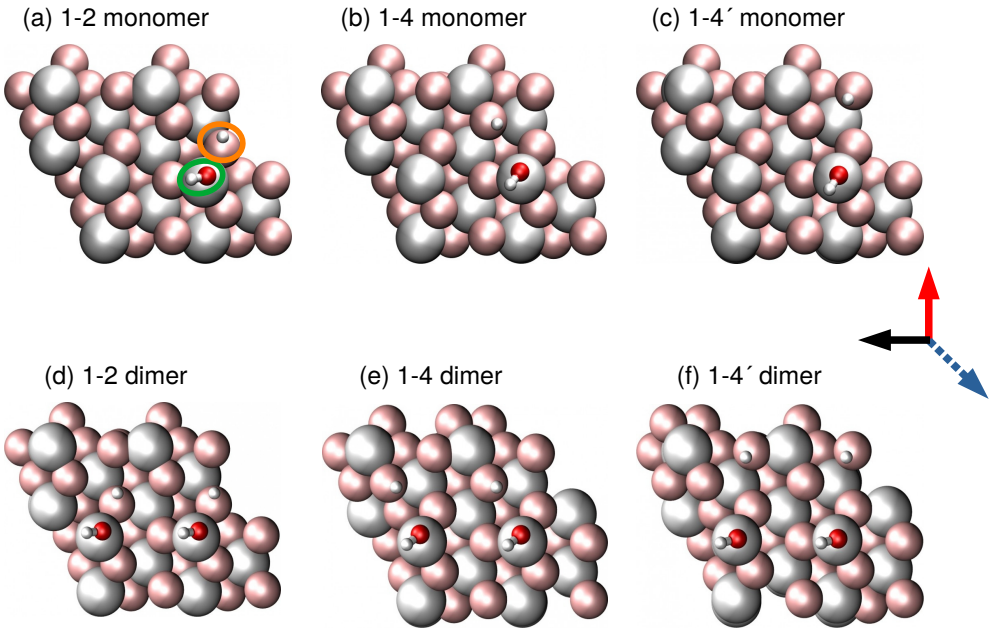

Figure 6: Top views of the dissociated D_2O species on Al-terminated α-$Al_2O_3(0001)$ (2×2) surface, used as starting geometries for AIMD. Dissociated species for coverage $1/4$ (one water molecule per cell) are in the upper panels: (a) 1-2 monomer, (b) 1-4 monomer, (c) 1-4' monomer. The lower panels show specific dimer models, for coverage $1/2$ (two water molecules per cell): (d) 1-2 dimer, (e) 1-4 dimer and (f) 1-4' dimer. All models consist of 9-layer surface supercells with additional water on top of the uppermost (Al) layer, with stoichiometric compositions of $Al_{24}O_{36}$ D_2O and $Al_{24}O_{36}(D_2O)_2$ for monomer and dimer cases, respectively. Optimized PBE+D2 structures are shown, with surface atoms visualized as "van-der-Waals spheres" in pale, while dissociated water molecules are shown in "ball-and-stick" representation (D in white, Al in grey and O in red). In what follows the water-hydroxyl groups are also denoted as "adsorbate OD" (circled in green), while OD groups consisting of a water-D plus a substrate O will be denoted as "surface OD" (circled in orange). For later reference, the Cartesian coordinate system used in this work is given by red (x-axis), black (y-axis) and blue (z-axis) arrows, the former in the surface plane, the latter perpendicular and pointing away from it.

are VSF experiments from Ref. [9], we list only OD-stretching modes in Table 1. We also show experimental values and corresponding assignments [9], as well as differences $\Delta\tilde{\nu} = \tilde{\nu} - \tilde{\nu}(\mathrm{OD}_{\mathrm{surf}}^{1-2})$ relative to the lowest-energy OD vibration, $\mathrm{OD}_{\mathrm{surf}}^{1-2}$. Our calculated NMA wavenumbers $\tilde{\nu}$ for coverage $1/4$ reproduce the harmonic values reported in Ref. [9], obtained at the same level of theory. As noticed there, there is a consistent and systematic red-shift of about 100 cm^{-1} of the theoretical OD-stretches compared to experimental ones. If we include anharmonicity along the normal modes in a quantum mechanical fashion (but no mode coupling) as done in Ref. [9], we get the values "AHO" (anharmonic oscillator) shown in the table. These indicate that the red-shift from experiment becomes even larger. However, we note that spacings between resonances

(measured by $\Delta\tilde{\nu}$) are quite similar between NMA/AHO theory and experiment, which was the basis for mode assignment in Ref. [9]. In particular, there are large frequency spacings between "adsorbed OD" and "surface OD" vibrations, with the latter being less energetic. (Referring to the mismatch in absolute wavenumbers, we mention that a significant improvement of OD stretching frequencies is achieved if scaling factors are used [16].)

Table 1: Comparison between vibrational (stretching) wavenumbers $\tilde{\nu}$ at the DFT/PBE+D2 level of theory and experimental results from Ref. [9] for dissociated D_2O on Al-terminated α-Al_2O_3(0001). $\Delta\tilde{\nu} = \tilde{\nu} - \tilde{\nu}(OD_{surf}^{1-2})$ gives resonance positions, relative to the lowest-frequency vibration, OD_{surf}^{1-2}. All wavenumbers are in cm^{-1}. Subscripts "surf" and "ads" denote "surface OD" and "adsorbate OD" as specified in the text. The theoretical values are for NMA (normal mode analysis), AHO (anharmonic oscillator treatment), and VDOS (vibrational density of states), the latter obtained from AIMD at 300 K.

	experiment[1]		theory, monomer						theory, dimer		
			NMA		AHO[1]		VDOS		NMA	VDOS	
assignment	$\tilde{\nu}$	$\Delta\tilde{\nu}$	$\tilde{\nu}$	$\Delta\tilde{\nu}$	$\tilde{\nu}$	$\Delta\tilde{\nu}$	$\tilde{\nu}_{max}$	$\Delta\tilde{\nu}$	$\tilde{\nu}$	$\tilde{\nu}_{max}$	$\Delta\tilde{\nu}$
OD_{surf}^{1-2}	2729±5	0	2629	0	2523	0	2596	0	2628, 2629	2607	0
OD_{surf}^{1-4}	2764±5	35	2647	18	2541	18	2636	40	2618, 2624	–[2]	–
$OD_{surf}^{1-4'}$	2790±3	61	2687	58	2583	60	2649	53	2693, 2694	2682	75
OD_{ads}^{1-4}	2900±7	171	2789	160	2696	171	2781	185	2780, 2781	2778	171
$OD_{ads}^{1-4'}$	2900±7	171	2789	160	2697	174	2780	184	2787, 2787	2778	171
OD_{ads}^{1-2}	2910±7	181	2804	175	2713	190	2795	199	2792, 2793	2788	181

[1] From Ref. [9]; [2] broad VDOS in this region.

In order to go beyond static DFT, we now report the results on VDOS curves calculated from AIMD trajectories at constant temperature (300 K). We started our AIMD trajectories from optimized PBE+D2 structures of dissociated species as shown in Fig.6. Initial velocities were generated randomly according to a Boltzmann distribution at $T = 300$ K. The equations of motion for nuclear degrees of freedom were propagated according to the Velocity-Verlet algorithm with timestep of $\Delta t = 0.2$ fs. We ran simulations for 50 ps in total. Technically, this was done by running five trajectories for each system, each of them being 10 ps long. Most of the propagation time was used for thermal equilibration, and only the last segment (2 ps) of each trajectory has been employed to sample the correlation functions.

In Fig.7, we show the VDOS for the three dissociated species in the "monomer" (coverage 1/4) and "dimer" (coverage 1/2) models when used as respective starting configurations in AIMD. In the upper panels of Fig.7, VDOS curves over a frequency range from 0 to 3000 cm^{-1} are shown, while the lower panels refer to the OD stretching region only, between 2500 and 3000 cm^{-1}.

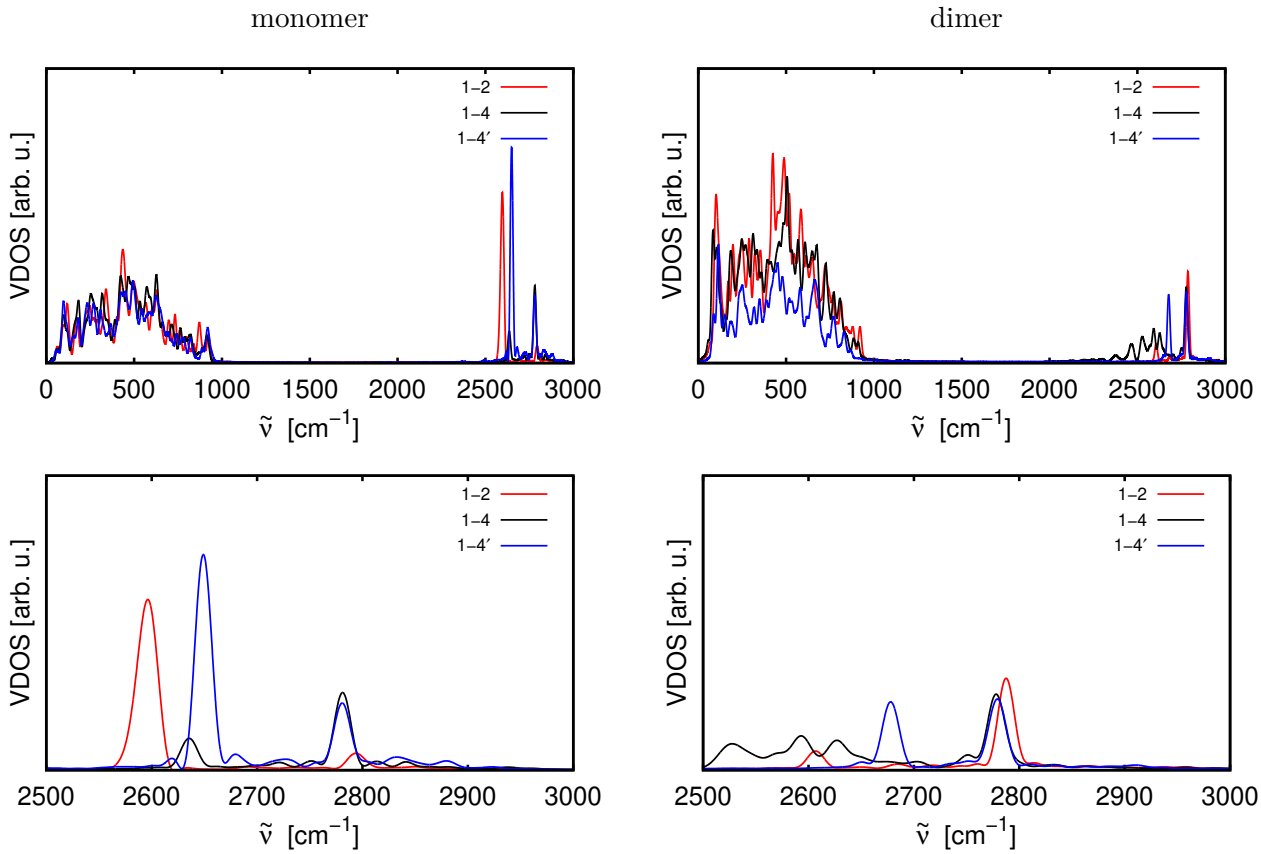

Figure 7: VDOS curves obtained by AIMD at 300 K, using the dissociated species 1-2, 1-4 and 1-4' for "monomers" (left) and "dimers" (right) of Fig.6 as starting configurations. Upper panels show the frequency range [0,3000] cm^{-1}, lower panels the OD stretching region [2500,3000] cm^{-1}. In the right panels, the VDOS scale is half that of the scale in the left panels.

It appears that the spectra for both triads of reaction products have two main bands. Up to 1000 cm^{-1} surface vibrations and OD bending modes are involved, while above 2500 cm^{-1} we see the signatures of different OD oscillators. For the "monomer" dissociated species, we have two maxima per model (1-2, 1-4 or 1-4'), *i.e.*, we retrieve all six modes reported in Tab.1. In the column "monomer, VDOS", we show the maxima of the VDOS curves as $\tilde{\nu}_{\max}$. Compared to the NMA results, we notice frequency shifts to lower values for all modes. In general, red-shifts are larger for "surface OD" than for "adsorbed" fragments. The red-shifts arise from anharmonicity of the potentialDa. (including an approximate treatment of mode coupling). Note that, due to the absence of vibrational energy quantization and zero-point energy, in classical dynamics only the low-energy portion of the potential is probed at 300 K, and therefore anharmonic corrections are underestimated w.r.t. to a quantum treatment (AHO) – for which a red-shift ~ 100 cm^{-1} was found above. For the "dimer", coverage 1/2 dissociative D_2O adsorption structures (right panels in Fig.7), a rather similar behaviour compared to the unimolecular example is found. In general,

the VDOS curves reflect the thermal motion of the adsorbates. This gives rise to new signals beyond NMA (most notably for the "1-4 dimer"), and to broadening of peaks beyond the energy resolution imposed by the finite propagation time.

The method of Ohto *et al* [17] allows for calculation of both first- (IR) and second-order (VSF) responses, which we have indeed done (Ref.(D) of Sec.5). Here we show only Sum Frequency spectra obtained from AIMD trajectories. Indeed, VSF spectra obtained from theory can be compared with experimental ones, which have been collected for D_2O on Al-terminated α-$Al_2O_3(0001)$ in Ref. [9]. The coverage was very low in these experiments, but not unequivocally defined as in our structural models. In Ref. [9], both *ppp*- and *ssp*-polarization schemes (and two experimental geometries) had been employed. Here we present theoretical VSF spectra for *ssp*, as obtained from $|\chi^{(2)}_{xxz}|^2$, a (squared) second-order suszeptibility element obtained from AIMD correlation functions. The results are shown in Fig. 8, for the monomer (left panel) and dimer (right panel) dissociated structures, respectively.

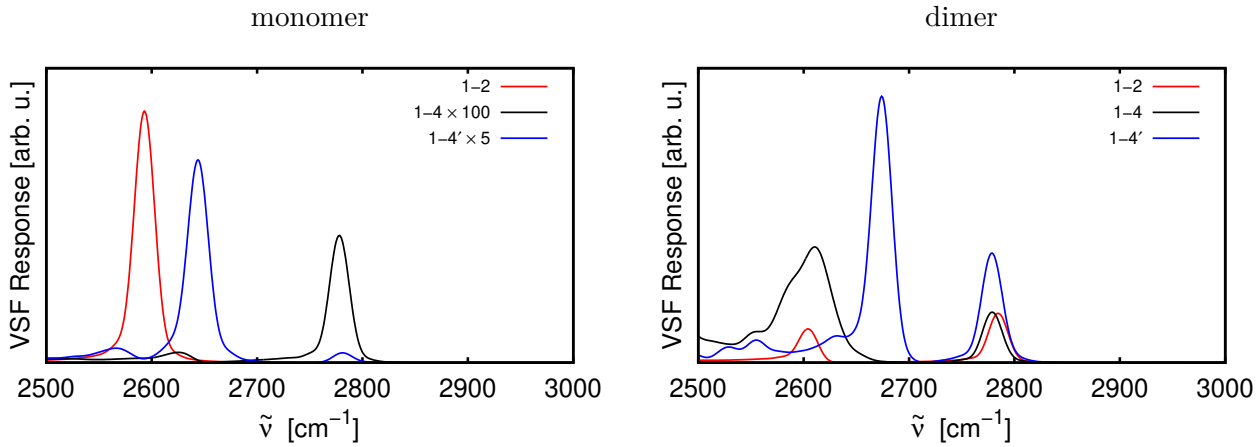

Figure 8: VSF signals representative for *ssp*-polarized experiments, obtained as $I^{\mathrm{VSF}}_{\mathrm{ssp}} \propto |\chi^{(2)}_{xxz}(\omega)|^2$. The left panel shows the VSF spectra for the "monomeric" dissociated species, while in right the panel spectra are shown for the "dimeric" dissociated models. For the left panel, scaling factors have been used as shown for 1-4 and 1-4', to make the figure clearer.

The spectra in the left panel show that the $\mathrm{OD}^{1-2}_{\mathrm{surf}}$ VSF signal at the *xxz*-polarization, around 2600 cm^{-1}, is by far the most intense. In fact, the $\mathrm{OD}^{1-2}_{\mathrm{ads}}$ peak at around 2800 cm^{-1}, which was slightly noticeable in the VDOS curves, is now not seen on the scale of Fig. 8 – it is about of factor 2000 weaker than $\mathrm{OD}^{1-2}_{\mathrm{surf}}$. For the 1-4 and 1-4' structures, both peaks (for surface and

adsorbate OD groups) are clearly seen in each case, however, their intensities are by far less intense than the OD_{ads}^{1-2} peak. For 1-4', around 2570 cm^{-1} a shoulder to the main peak at 2640 cm^{-1} is found, which could be assigned to a fluctuating hydrogen bonded vibration between the two OD fragments. We note that VSF intensities have to be taken with care, since no weighting with the (unknown) population of each species (Boltzmann or non-Boltzmann) was made, *i.e.*, strictly, only intensities for a given model (*e.g.*, OD_{ads}^{1-2} with OD_{surf}^{1-2}) can be compared to each other.

In the experiment [9] (with the aid of NMA from theory), at the *spp*-polarization, resonances for $OD_{surf}^{1-4'}$, OD_{ads}^{1-4} and $OD_{ads}^{1-4'}$ (the latter two merged in one peak), and OD_{ads}^{1-2} have been assigned, with the latter being the most intense, and $OD_{surf}^{1-4'}$ being the least intense. With a different geometry and *ppp*-polarization, resonances for the "surface OD" species, OD_{surf}^{1-2}, OD_{surf}^{1-4}, and $OD_{surf}^{1-4'}$ were reported. The comparison of calculated VSF spectra with experimental ones is somewhat tricky. In fact, while peak positions and relative frequencies of resonances are in reasonably good agreement with experiment, as well as spectral linewidths around 20 cm^{-1}, absolute vibrational frequencies and intensities are not directly relatable to the ones reported in Ref. [9]. Possible reasons of mismatch are first imputable to the choice of adsorbed D_2O models on the (0001) surface. In fact, while in theory we have assumed a perfect adsorption structure for each given coverage value (either 1/4 or 1/2), in experiment the absolute coverage was probably lower but the local formation of water clustering and islands could not be excluded *a priori*. Other possible causes of deviation between theory and experiment are discussed in Ref.(D) of Sec.5.

3 Aims for the new funding period

In the following section we describe our plans for conclusive simulations about the water / α-Al_2O_3(0001) interface for the last funding period, as well as for new possible research lines connected to this project.

Subproject 4: Water thin-film structures and vibrational dynamics at OH-terminated α-Al_2O_3(0001): From structural properties to vibrational signatures using continuum solvation models

In the last proposal we aimed at extending the computational methodology used in subproject 2. In order to improve the analysis of water interactions and dynamics on α-Al_2O_3(0001) surface in ambient conditions, a systematic study of higher coverage models was desirable, until the full (bulk) water / solid interface was considered. However, instead of performing computationally heavy DFT / AIMD calculations with increasing water coverages, our idea has been directed to improve the description of interfacial properties at the electronic structure level by including implicit solvation models. That means improving the simulation of H_2O / α-alumina interactions

employing an indirect, yet fully quantum-mechanical treatment of the aqueous environment with a polarizable continuum model (PCM). Recent developments allow for such treatment also for periodic systems, as R. Hennig and coworkers [20, 21] demonstrated with the *VASPsol* package implementation.

Initial tests conducted by our group on local cluster machines using this method [20, 21] have shown that for insulating systems as α-Al_2O_3, these calculations are extremely sensitive to dipolar corrections. In fact, even using the conventional dipole corrections for VASP, yet employing a single slab model for the (0001) surface, the implicit solvent generates an unphysical description of electrostatics at the interface, which may cause artificial surface reconstructions or unreasonable adsorption energies.

Now, thanks to these better insights, we aim at applying the *VASPsol* method again to describe how improved solvation of the (0001) surface can affect structural properties, vibrational signatures and dynamics of adsorbed water within AIMD at finite temperature. For this purpose we will rely on double slab symmetric models with larger surface thickness, which avoid the inclusion of dipolar corrections, already yielding qualitatively good results in terms of solvation energies for different models.

Outlook subproject: Dynamics of different adsorbate / surface systems from periodic DFT and AIMD simulations

Eventually, this last proposal for project bbc00001 should also prepare the way for new research conducted in our group, which will rely on the same methodological framework of periodic DFT and AIMD simulations. In particular, other adsorbate / surface systems shall be investigated, for instance H / Si(100) [22] and CO / Cu(100) [23], which have been already object of complementary studies by our group, using either quantum or classical (Langevin) dynamics based on parametrized Hamiltonians and / or pre-calculated Potential Energy Surfaces. The investigation of these systems would greatly benefit from DFT-based AIMD simulations at finite temperature. In particular, vibrational relaxation of Si-H and Si-D bending modes for H / Si(100) proceed on ps (for H) or sub-ps (for D) timescales [22], and should therefore be accessible by AIMD. On the long run, theoretical vibrational spectroscopy based on AIMD trajectories and velocity-velocity autocorrelation functions are desirable, also for this system.

4 Planned calculations and requested resources

As mentioned above and in the previous proposal, we will continue performing our calculations with the Vienna ab initio Simulation Package (VASP) [2, 3], using the similar settings as before. On the DFT level of theory, the PBE functional shall be still employed while both Grimme's dispertion corrections D2 and D3 shall be tested. Other functionals, especially to test the validity of continuum solvation models may also be used.
For AIMD simulations in the canonical ensemble, thermalization will be still done with the Nosé-Hoover thermostat [10]. Such calculations are to be done on 6 or 8 nodes (144 or 192 CPUs) of mpp2 as we carried out in the previous funding period. Based on the simulations carried out in the past, we found on average a computing time of 140 NPL per ps of simulation, for the systems studied so far in subproject 2. Since the systems to be studied in the coming period are of similar complexity, we use the following "counting unit" for measuring the expected effort of our calculations: **1 ps AIMD simulation time = 140 NPL**. As shown above, in order to achieve converge spectroscopic signals and properly sampled trajectories, the typical AIMD propagation time shall be 10-20 ps for each trajectory.

Specifically, the following calculations are planned:

1. *Subproject 4: From structural properties to vibrational signatures using continuum solvation models.*

   Additional AIMD calculations in the canonical ensemble (300 K) using a combined GGA-level DFT and polarizable continuum approach (*VASPsol*) are planned for the HS+2ML system in order to investigate the effects of bulk water solvation on vibrational spectra.

   For such calculations we plan to employ at least a new structural model using symmetric slab for the hydroxylated (0001) surface. Different models will be investigated to address the effect played by water coverage and increasing hydrogen bonding. We expect to run 10 trajectories for each system, where every trajectory shall include a thermalization phase in the NVT ensemble and a production run for vibrational spectra and dynamical processes in the NVE ensemble. Taking at least 15 ps for each entire trajectory and five structural models, around **750 ps** are needed to complete the project.

2. *Outlook subproject: Dynamics of different adsorbate / surface systems from periodic DFT and AIMD simulations.*

   Further calculations, both dynamical and stationary (*e.g.*, for geometry optimization and NMA or test calculations for new structures) are needed. We will concentrate on the H/Si(100) system [22], with elementary cells of similar complexity as for the H_2O/Al_2O_3

case. We estimate an "equivalent effort" corresponding to **200 ps**.

Altogether, the expected effort is therefore 950 ps, corresponding to **950 × 140 NPL = 133 kNPL**. The requested 133 kNPL should be distributed over the coming four quarters as:

quarter	I	II	III	IV
NPL estimated	60 000	20 000	20 000	33 000

5 References to papers related to project *bbc00001*

(A) Sophia Heiden, Jonas Wirth, R. Kramer Campen and Peter Saalfrank. Water Molecular Beam Scattering at α-Al_2O_3(0001): An *Ab Initio* Molecular Dynamics Study, *The Journal of Physical Chemistry C*, 122, 15494-15504 (2018).

(B) Giacomo Melani, Yuki Nagata, Jonas Wirth and Peter Saalfrank. Vibrational Spectroscopy of Hydroxylated α-Al_2O_3(0001) Surfaces with and without Water: An *Ab Initio* Molecular Dynamics Study, *The Journal of Chemical Physics*, 149, 014707:1-10 (2018).

(C) Sophia Heiden, Denis Usvyat and Peter Saalfrank. Theoretical Surface Science Beyond Gradient-Corrected Density Functional Theory: Water at α-Al_2O_3(0001) as a Case Study, *The Journal of Physical Chemistry C*, 123, 6675-6684 (2019).

(D) Giacomo Melani, Yuki Nagata, R. Kramer Campen and Peter Saalfrank. Vibrational Spectra of Dissociatively Adsorbed D_2O on Al-terminated α-Al_2O_3(0001) Surfaces from Ab Initio Molecular Dynamics, submitted to J. Chem. Phys. (2019).

References

[1] W. Kohn and L. J. Sham. Self-consistent equations including exchange and correlation effects. *Phys. Rev.*, 140:1133–1138, (1965).

[2] G. Kresse and J. Hafner. *Ab initio*, molecular dynamics for liquid metals. *Phys. Rev. B*, 47(1):558–561, (1993).

[3] G. Kresse and J. Hafner. *Ab initio*, molecular dynamics for open-shell transition metals. *Phys. Rev. B*, 48(17):13115–13118, (1993).

[4] J. P. Perdew, K. Burke, and M. Ernzerhof. Generalized gradient approximation made simple. *Phys. Rev. Lett.*, 77(18):3865–3868, (1996).

[5] P. E. Blöchl. Projector augmented-wave method. *Phys. Rev. B*, 50(24):17953–17979, (1994).

[6] G. Kresse and D. Joubert. From ultrasoft pseudopotentials to the projector augmented-wave method. *Phys. Rev. B*, 59(3):1758–1775, (1999).

[7] S. Grimme. Semiempirical GGA-type density functional constructed with a long-range dispersion correction. *J. Comp. Chem.*, 27(15):1787–1799, (2006).

[8] J. Wirth and P. Saalfrank. The chemistry of water on α-alumina: Kinetics and nuclear quantum effects from first principles. *J. Phys. Chem. C*, 116(51):26829–26840, (2012).

[9] H. Kirsch, J. Wirth, Y. Tong, M. Wolf, P. Saalfrank, and R. K. Campen. Experimental characterization of unimolecular water dissociative adsorption on α-alumina. *J. Phys. Chem. C*, 118(25):13623–13630, (2014).

[10] Shūichi Nosé. A molecular dynamics method for simulations in the canonical ensemble. *Mol. Phys.*, 52(2):255–268, (1984).

[11] G. Melani, Y. Nagata, J. Wirth, and P. Saalfrank. Vibrational spectroscopy of hydroxylated α-Al_2O_3(0001) surfaces with and without water: An ab initio molecular dynamics study. *J. Chem. Phys.*, 149(1):014707, (2018).

[12] Y. Nagata, S. Yoshimune, C.-S. Hsieh, J. Hunger, and M. Bonn. Ultrafast vibrational dynamics of water disentangled by reverse nonequilibrium ab initio molecular dynamics simulations. *Phys. Rev. X*, 5:021002, (2015).

[13] J. Jeon, J. H. Lim, S. Kim, H. Kim, and M. Cho. Simultaneous spectral and temporal analyses of kinetic energies in nonequilibrium systems: Theory and application to vibrational relaxation of O-D stretch mode of HOD in water. *The Journal of Physical Chemistry A*, 119(21):5356–5367, (2015).

[14] J. Jeon, C.-S. Hsieh, Y. Nagata, M. Bonn, and M. Cho. Hydrogen bonding and vibrational energy relaxation of interfacial water: A full DFT molecular dynamics simulation. *J. Chem. Phys.*, 147(4):044707, (2017).

[15] D. Lesnicki and M. Sulpizi. A microscopic interpretation of pumpâprobe vibrational spectroscopy using ab initio molecular dynamics. *J. Phys. Chem. B*, 122(25):6604–6609, (2018).

[16] S. Heiden, J. Wirth, R. K. Campen, and P. Saalfrank. Water molecular beam scattering at α-Al_2O_3(0001): An ab initio molecular dynamics study. *J. Phys. Chem. C*, 122(27):15494–15504, (2018).

[17] T. Ohto, K. Usui, T. Hasegawa, M. Bonn, and Y. Nagata. Toward ab initio molecular dynamics modeling for sum-frequency generation spectra; an efficient algorithm based on surface-specific velocity-velocity correlation function. *J. Chem. Phys.*, 143(12):124702, (2015).

[18] T. Kurita, K. Uchida, and A. Oshiyama. Atomic and electronic structures of α-Al_2O_3 surfaces. *Phys. Rev. B*, 82(15):155319, (2010).

[19] S. Heiden, D. Usvyat, and P. Saalfrank. Theoretical surface science beyond gradient-corrected density functional theory: Water at α-Al_2O_3(0001) as a case study. *J. Phys. Chem. C*, 123(11):6675–6684, (2019).

[20] M. Fishman, H. L. Zhuang, K. Mathew, W. Dirschka, and R. G. Hennig. *Phys. Rev. B.*, 87:245402, (2013).

[21] K. Mathew, R. Sundararaman, K. Letchworth-Weaver, T. A. Arias, and R. G. Hennig. *J. Chem. Phys.*, 140:084106, (2014).

[22] F. Bouakline, U. Lorenz, G. Melani, G. K. Paramonov, and P. Saalfrank. Isotopic effects in vibrational relaxation dynamics of H on a Si(100) surface. *J. Chem. Phys.*, 147(14):144703, (2017).

[23] R. Marquardt, F. Cuvelier, R. A. Olsen, E. J. Baerends, J. C. Tremblay, and P. Saalfrank. A new analytical potential energy surface for the adsorption system co/cu(100). *J. Chem. Phys.*, 132(7):074108, (2010).